Organometallics **2008,** *27,* 6178–6187

Bimetallic Calcium and Zinc Complexes with Bridged *β*-Diketiminate Ligands: Investigations on Epoxide/CO$_2$ Copolymerization

Dirk F.-J. Piesik, Sven Range, and Sjoerd Harder*

Anorganische Chemie, Universität Duisburg-Essen, Universitätsstraße 5−7, 45117 Essen, Germany

Received June 27, 2008

A series of dinucleating *bis*(β-diketiminate) ligands with rigid bridges has been prepared. In all cases the β-diketiminate unit is 2,6-iPr$_2$C$_6$H$_3$NC(Me)C(H)C(Me)N-(bridge), and the bridges are either *para*-phenylene, *meta*-phenylene or 2, 6-pyridylene (the dinucleating ligands are abbreviated as PARA-H$_2$, META-H$_2$ and PYR-H$_2$, respectively). These ligands have been converted to heteroleptic bimetallic calcium and zinc complexes. For calcium, only the PARA-phenylene bridged ligand led to a heteroleptic bimetallic calcium amide complex PARA-[CaN(SiMe$_3$)$_2$·THF]$_2$. For the other ligands, homoleptic complexes have been isolated: META-Ca and PYR-Ca. For zinc, the whole range of heteroleptic amides could be isolated: PARA-[ZnN(SiMe$_3$)$_2$]$_2$, META-[ZnN(SiMe$_3$)$_2$]$_2$, and PYR-[ZnN(SiMe$_3$)$_2$]$_2$. Analogue ethylzinc complexes have been prepared in quantitative yields: PARA-(ZnEt)$_2$, META-(ZnEt)$_2$, and PYR-(ZnEt)$_2$. Reactions of the ethylzinc complexes with SO$_2$ gave access to the ethylsulfinate complexes META-(ZnO$_2$SEt)$_2$ and PYR-(ZnO$_2$SEt)$_2$; for the *para*-phenylene bridged ligand no products could be isolated. Crystal structures of the following complexes are presented: (META-Ca)$_2$, PARA-[CaN(SiMe$_3$)$_2$·THF]$_2$, PARA-[ZnN(SiMe$_3$)$_2$]$_2$, META-[ZnN(SiMe$_3$)$_2$]$_2$, PYR-(ZnEt)$_2$, and PYR-(ZnO$_2$SEt)$_2$. All heteroleptic complexes have been tested for activity in the copolymerization of cyclohexene oxide (CHO) and CO$_2$. The bimetallic complex PARA-[CaN(SiMe$_3$)$_2$·THF]$_2$ is not active. For zinc, the PARA and META complexes were found to be active under highly concentrated conditions (Zn/CHO ratio of 1/1000; no solvent), but no significant polymer yields could be achieved with PYR complexes. This is either due to conformational changes of the complex or to coordination of the pyridylene N atom to the catalytic centers. The order of activity found in the bimetallic zinc complexes is META > PARA. This is likely due to a more advantageous Zn···Zn distance in the *meta*-phenylene bridged bimetallic catalysts. There are several indications for bimetallic action. First of all, the ethylzinc systems PARA-(ZnEt)$_2$ and META-(ZnEt)$_2$ initiate CHO/CO$_2$ copolymerization, whereas monometallic ethylzinc catalysts are not reactive. Second, the bimetallic zinc catalysts are also highly active under diluted conditions: a low metal/CHO ratio of 1/3000 gave high-MW polymers (M_n > 100.000, PDI = 1.33) with essentially only carbonate linkages. In contrast, monometallic systems show a drastic loss of activity upon dilution. Finally, the bimetallic catalyst META-[ZnN(SiMe$_3$)$_2$]$_2$ shows a significantly higher activity than a comparable monometallic model system.

Introduction

As the need for biodegradable polymers from biorenewable feedstocks is becoming urgent,[1] research on the alternating epoxide/CO$_2$ copolymerization is rapidly increasing.[2,3] Notably, Coates' landmark discovery of highly active homogeneous Zn catalysts[4] for high molecular weight polycarbonates has led to a boost in research activities.

These catalysts in question are composed of a bulky β-diketiminate ligand, chelating the Zn center, and an initiating group that can be (Me$_3$Si)$_2$N$^-$, an alkoxide, or acetate. Alkyl groups such as Et are not active, however, can be conveniently converted to ethylsulfinates (EtSO$_2{}^-$), which are highly active initiators.[5] There is ample evidence for a bimetallic mechanism with a carboxylate end group as the resting state (epoxide insertion is the rate-determining step; Scheme 1).[4] It has been shown that the intermediate carboxylate species are in a monomer−dimer equilibrium that is highly sensitive toward the nature of the aryl subtituents in the β-diketiminate ligand. As

---

* To whom correspondence should be sent. E-mail: sjoerd.harder@uni-due.de.

(1) (a) Chisholm, M. H.; Zhou, Z. *J. Mater. Chem.* **2004**, *14*, 3081–3092. (b) Domb, A. J. *Polymer Prepr.* **2007**, *48*, 640. (c) van Beilen, J. B.; Poirier, Y. *Plant J.* **2008**, *54*, 684–701.

(2) Recent reviews: (a) Darensbourg, D. J.; Holtcamp, M. W. *Coord. Chem. Rev.* **1996**, *153*, 155–174. (b) Darensbourg, D. J.; Mackiewicz, R. M.; Phelps, A. L.; Billodeaux, D. R. *Acc. Chem. Res.* **2004**, *37*, 836–844. (c) Sugimoto, H.; Inoue, S. *J. Polym. Sci., Part A: Polym. Chem.* **2004**, *42*, 5561–5573. (d) Coates, G. W.; Moore, D. R. *Angew. Chem.* **2004**, *116*, 6784−6806; (e) Coates, G. W.; Moore, D. R. *Angew. Chem. Int. Ed.* **2004**, *43*, 6618−6639.

(3) (a) Darensbourg, D. J.; Holtcamp, M. W. *Macromolecules* **1995**, *28*, 7577–7579. (b) Super, M.; Berluche, E.; Costello, C.; Beckman, E. *Macromolecules* **1997**, *30*, 368–372. (c) Darensbourg, D. J.; Holtcamp, M. W.; Struck, G. E.; Zimmer, M. S.; Niezgoda, S. A.; Rainey, P.; Robertson, J. B.; Draper, J. D.; Reibenspies, J. H. *J. Am. Chem. Soc.* **1999**, *121*, 107–116.

(4) (a) Cheng, M.; Lobkovsky, E. B.; Coates, G. W. *J. Am. Chem. Soc.* **1998**, *120*, 11018–11019. (b) Cheng, M.; Moore, D. R.; Reczek, J. J.; Chamberlain, B. M.; Lobkovsky, E. B.; Coates, G. W. *J. Am. Chem. Soc.* **2001**, *123*, 8738–8749. (c) Moore, D. R.; Cheng, M.; Lobkovsky, E. B.; Coates, G. W. *J. Am. Chem. Soc.* **2003**, *125*, 11911–11924.

(5) Eberhardt, R.; Allmendinger, M.; Luinstra, G. A.; Rieger, B. *Organometallics* **2003**, *22*, 211–214.

10.1021/om800597f CCC: $40.75

Scheme 1

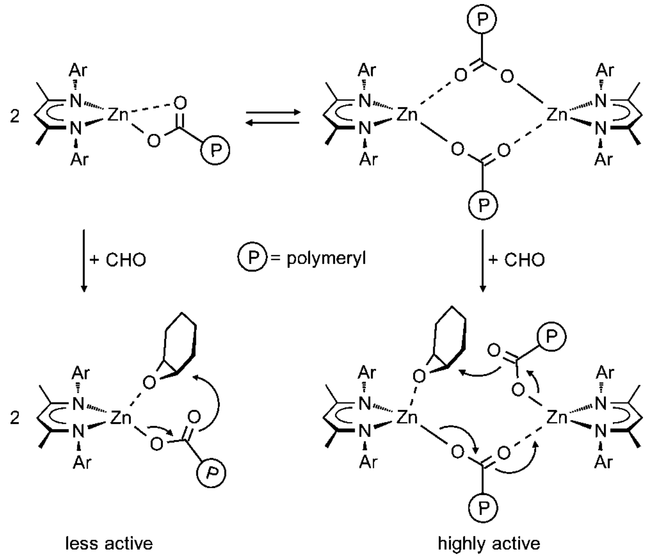

the dimer is the prominent active species,[6] the activities of the polymerization catalysts can be controlled by small variations in the *β*-diketiminate ligands. Also, catalyst concentration is a decisive factor for activity: at very low concentration the monomer−dimer equilibrium is shifted to the monomeric side and hardly any catalytic activity can be observed.[7,9,16] This is a serious drawback since monomer-to-polymer conversion is generally limited on account of viscosity problems.[7−9] Dilution of the system by either addition of monomer or an inert solvent would shift the monomer−dimer equilibrium to the monomeric side, thus reducing catalyst activity.

Recent research focuses on the introduction of dinucleating ligands (**1**−**3**) that circumvent the equilibrium between the active dimer and inactive (or less active) monomer. The dinuclear Zn catalyst **1** has been shown to be highly active for the copolymerization of CHO and CO_2.[7] Even under very diluted conditions, high molecular weight polymers (M_n up to 284 000) could be obtained. Dinuclear Zn complexes based on parallel *β*-diketiminate ligands (**2**) were only moderately active, probably on account of overcrowding in the reaction pocket.[10] A bimetallic Zn complex with the Trost ligand (**3-Zn**) has been shown to be active in CHO/CO_2 copolymerization in diluted solutions and under the remarkably low CO_2 pressure of 1 bar.[11] Interestingly, the analogue dinuclear Mg complex **3-Mg** was also found to be active in CHO/CO_2 copolymerization.[12]

Scheme 2. Reagents and conditions: (i) $[Et_3O]^+[BF_4]^-$, CH_2Cl_2, 20 °C; (ii) Et_3N and diamine, 20 °C

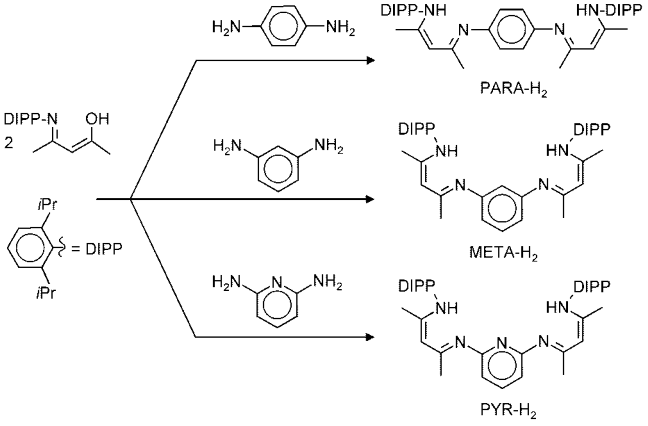

Because the use of calcium reagents in catalysis is one of our main research areas,[13] we are interested in exploring their potential in the alternating CHO/CO_2 copolymerization. Although well-defined calcium catalysts have recently been introduced for the ring opening polymerization of polar monomers such as lactides and cyclic carbonates,[14] hitherto no calcium catalysts have been reported for CHO/CO_2 copolymerization. It is highly likely that, similar to the Zn catalysts, a bimetallic mechanism could be operative. Therefore, we directed our research to the syntheses of dinuclear complexes of calcium and zinc. Dinucleating *bis*(salicylaldimide) ligands were found to be unsuitable in the stabilization of bimetallic calcium or zinc amides.[15] We now introduce a set of dinucleating ligands based on the bulkier *β*-diketiminate unit with a variety of rigid bridges and evaluate the possibility of obtaining heteroleptic bimetallic calcium and zinc complexes. The use of these complexes in CHO/CO_2 copolymerization and the influences of the bridging units will be discussed.

Results and Discussion

Dinucleating Ligands. Three bridged *β*-diketiminate ligands have been prepared in reasonable yields by a two-step standard condensation route given in Scheme 2. The diprotic ligands are abbreviated according to the nature of the bridging unit: 1,4-phenylene (PARA-H_2), 1,3-phenylene (META-H_2), or 2,6-pyridylene (PYR-H_2). The dinucleating ligands PYR and META allow for a wide range of metal···metal distances (2.5−8 Å), whereas the metal···metal distances in a bimetallic complex with the PARA ligand lies in the range of approximately 5.5−8.5 Å.[16] The PYR ligand is a potential pentadentate ligand and has been incorporated to study the effect of additional metal coordination.

Bimetallic Calcium Complexes. Two-fold deprotonation of PARA-H_2 with two equivalents of $[(Me_3Si)_2N]_2Ca\cdot(THF)_2$ gave exclusively the heteroleptic complex PARA-$[CaN(SiMe_3)_2\cdot THF]_2$ in a reasonable yield (Scheme 3). This bimetallic complex is also, in benzene solution, stable toward ligand exchange, and the Schlenk equilibrium is fully at the heteroleptic side. Deprotonation of META-H_2 with two equivalents of $[(Me_3Si)_2N]_2Ca\cdot(THF)_2$ in either benzene or THF gave a mixture of heteroleptic META-$[CaN(SiMe_3)_2\cdot(THF)_x]_2$ and

---

(6) There are indications that also the monomeric species is active in epoxide/CO_2 copolymerization, albeit with much slower conversion rates.[4c,5]

(7) Lee, B. Y.; Kwon, H. Y.; Lee, S. Y.; Na, S. J.; Han, S.; Yun, H.; Lee, H.; Park, Y.-W. *J. Am. Chem. Soc.* **2005**, *127*, 3031–3037.

(8) Cohen, C. T.; Thomas, C. M.; Peretti, K. L.; Lobkovsky, E. B.; Coates, G. W. *Dalton Trans.* **2006**, 237–249.

(9) van Meerendonk, W. J.; Duchateau, R.; Koning, C. E.; Gruter, G.-J. M. *Macromol. Rapid Commun.* **2004**, *25*, 382–386.

(10) Pilz, M. F.; Limberg, C.; Lazarov, B. B.; Hultzsch, K. C.; Ziemer, B. *Organometallics* **2007**, *26*, 3668–3676.

(11) Xiao, Y.; Wang, Z.; Ding, K. *Chem.—Eur. J.* **2005**, *11*, 3668–3678.

(12) Xiao, Y.; Wang, Z.; Ding, K. *Macromolecules* **2006**, *39*, 128–137.

(13) (a) Harder, S.; Feil, F.; Knoll, K. *Angew. Chem., Int. Ed.* **2001**, *40*, 4261–4264. (b) Buch, F.; Brettar, J.; Harder, S. *Angew. Chem., Int. Ed.* **2006**, *45*, 2741–2745.

(14) (a) Chisholm, M. H.; Gallucci, J.; Phomphrai, K. *Chem. Commun.* **2003**, 48–49. (b) Zhong, Z.; Schneiderbauer, S.; Dijkstra, P. J.; Westerhausen, M.; Feijen, J. *J. Polym. Bull.* **2003**, *51*, 175–182. (c) Chisholm, M. H.; Gallucci, J.; Phomphrai, K. *Inorg. Chem.* **2004**, *43*, 6717–6725. (d) Darensbourg, D. J.; Choi, W.; Ganguly, P.; Richers, C. P. *Macromolecules* **2006**, *39*, 4374–4379.

(15) Range, S.; Piesik, D. F.-J.; Harder, S. *Eur. J. Inorg. Chem.* **2008**, *22*, 3442–3451..

(16) This range of metal···metal distances is based on simple geometrical calculations using a general M−O and M−N distance of 2.5 Å and allowing for rotation around the N−C(bridge) bonds.

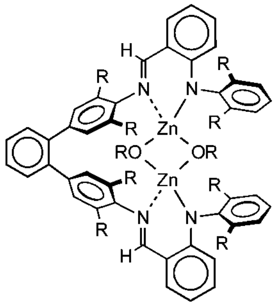

1

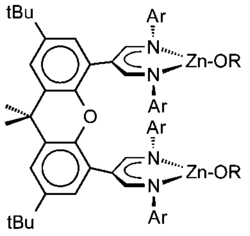

2

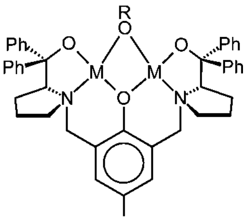

3-M

Scheme 3. Syntheses of Bimetallic Ca and Zn Complexes

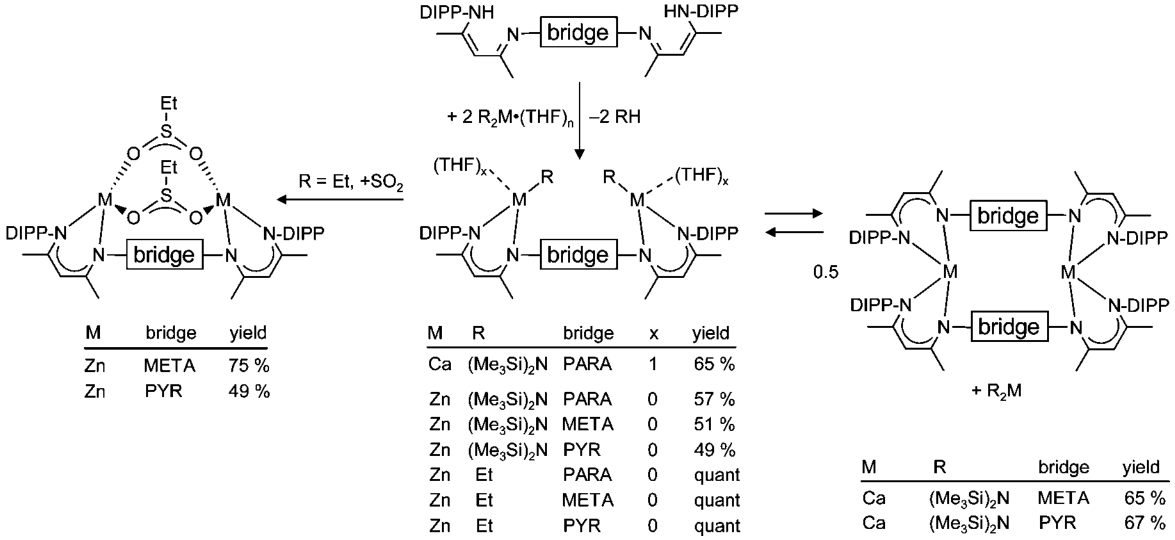

M	bridge	yield
Zn	META	75 %
Zn	PYR	49 %

M	R	bridge	x	yield
Ca	$(Me_3Si)_2N$	PARA	1	65 %
Zn	$(Me_3Si)_2N$	PARA	0	57 %
Zn	$(Me_3Si)_2N$	META	0	51 %
Zn	$(Me_3Si)_2N$	PYR	0	49 %
Zn	Et	PARA	0	quant
Zn	Et	META	0	quant
Zn	Et	PYR	0	quant

M	R	bridge	yield
Ca	$(Me_3Si)_2N$	META	65 %
Ca	$(Me_3Si)_2N$	PYR	67 %

homoleptic (META-Ca)$_2$. The homoleptic dimer (META-Ca)$_2$ could be obtained in crystalline purity. For the pyridylene-bridged ligand, the Schlenk equilibrium was found to be completely to the homoleptic side and only (PYR-Ca)$_x$ could be observed and isolated. The crystal structures of the complexes PARA-[CaN(SiMe$_3$)$_2$•THF]$_2$ and (META-Ca)$_2$ are described below.

Bimetallic Zinc Complexes. Reactions of the dinucleating ligands with [(Me$_3$Si)$_2$N]$_2$Zn gave in all cases good yields of the heteroleptic complexes PARA-[ZnN(SiMe$_3$)$_2$]$_2$, META-[ZnN(SiMe$_3$)$_2$]$_2$, and PYR-[ZnN(SiMe$_3$)$_2$]$_2$. Deprotonation with Et$_2$Zn gave quantitative conversion to PARA-(ZnEt)$_2$, META-(ZnEt)$_2$, and PYR-(ZnEt)$_2$. In all cases the complexes are completely stable against ligand exchange reactions and the Schlenk equilibrium is not an issue. The heteroleptic ethylzinc compounds PYR-(ZnEt)$_2$ and META-(ZnEt)$_2$ cleanly reacted with SO$_2$ to form ethylsulfinate complexes. Reaction of PARA-(ZnEt)$_2$ with SO$_2$ gave a mixture of unidentified products. Crystal structures for PARA-[ZnN(SiMe$_3$)$_2$]$_2$, META-[ZnN(SiMe$_3$)$_2$]$_2$, PYR-(ZnEt)$_2$, and PYR-(ZnO$_2$SEt)$_2$ are described below.

Crystal Structures. META-Ca crystallizes as a crystallographically C_2-symmetric dimer (Figure 1). The Ca^{2+} ions are 4-fold coordinated by two N,N-chelating β-diketiminate units. These β-diketiminate units coordinate in significantly different fashions. One of the ligands binds face-on to Ca (N1, N2). This allows for a slightly bonding contact to the central carbon atom C3 (2.841(5) Å), which on account of charge delocalization is significantly negatively charged. The other ligand (N3, N4) coordinates edge-on, and the Ca^{2+} ion is situated in the NCCCN plane. These fundamentally different coordination modes affect neither the Ca−N bond distances nor the geometry of the NCCCN backbone.

PARA-[CaN(SiMe$_3$)$_2$•THF]$_2$ crystallizes as a crystallographically C_2-symmetric complex (Figure 2) in which each Ca^{2+} ion is bound to a β-diketiminate unit, a (Me$_3$Si)$_2$N$^-$ ligand and a THF ligand. The distorted tetrahedral coordination sphere is further filled with an agostic interaction between Ca and C25 (3.315(4) Å). The latter weak interaction is also evident from the asymmetric coordination of the (Me$_3$Si)$_2$N$^-$ ligand; the

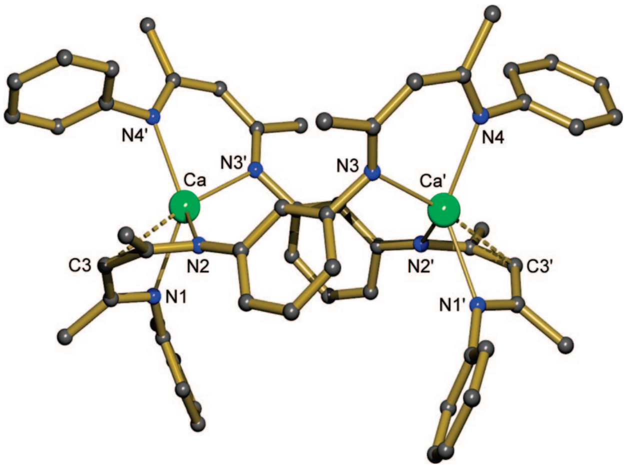

Figure 1. Crystal structure of [META-Ca]$_2$ (viewed perpendicular on the vertically oriented C_2-axis). For clarity, hydrogen atoms and *i*Pr-substituents have been omitted. Selected bond distances in Å: Ca−N1 2.326(3), Ca−N2 2.302(3), Ca−N3′ 2.300(3), Ca−N4′ 2.366(3), Ca−C3 2.841(5), and Ca•••Ca′ 7.017(2).

Ca−N3−Si2 angle of 110.8(1)° is significantly smaller than the angle Ca−N3−Si1 of 119.8(1)°. The bond distances to Ca correspond well to those observed in the comparable unbridged complex **4**.[14c]

PARA-$[ZnN(SiMe_3)_2]_2$ crystallizes as a complex of approximate (noncrystallographic) C_2-symmetry (Figure 3). The tricoordinate Zn atoms are situated at opposite sides of the bridge plane. The metal coordination geometry and the bond distances to the zinc atoms are very similar to those in the mononuclear species **5**.[4b]

META-$[ZnN(SiMe_3)_2]_2$ crystallizes, similar to PARA-$[ZnN(SiMe_3)_2]_2$, as an approximately C_2-symmetric complex (Figure 4). The tricoordinate Zn atoms are situated at opposite sides of the bridge plane. The metal coordination geometry and the bond distances to the zinc atoms do not differ significantly from those observed in PARA-$[ZnN(SiMe_3)_2]_2$. The only notable difference is the Zn···Zn distance (6.098(2) Å), which is shorter than that in PARA-$[ZnN(SiMe_3)_2]_2$ (8.173(2) Å).

PYR-$(ZnEt)_2$ crystallizes as a nonsymmetric complex in which the dinucleating ligand possesses approximate (noncrystallographic) C_s-symmetry (Figure 5). The tricoordinate Zn atoms are situated at the same side of the bridge plane and there are no evident pyridyl-Zn interactions. Bond distances to the Zn atoms are similar to those in the mononuclear complex **6**.[17]

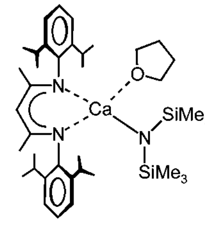

4

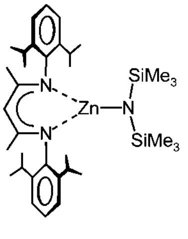

5

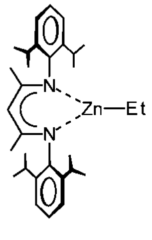

6

PYR-$(ZnO_2SEt)_2$ crystallizes as a monomeric complex of approximate (noncrystallographic) C_2-symmetry (Figure 6). The Zn atoms are bridged by the two $EtSO_2^-$ ligands and show distorted tetrahedral coordination. There is, however, indication for an additional weak interaction between the pyridyl bridge and the metal centers. In general, the NCCCN-plane of the β-diketiminate unit is typically oriented perpendicular to the plane of the bridging ring. In the current structure, however, interplanar angles of 31.5(1)° and 40.1(1)° are observed. This is likely due to attracting forces between the metal centers and the pyridylene nitrogen atom. The ligand geometry also results in repulsion between the Me substituent and the bridge and gives rise to rather acute N−C−N angles (N2−C−N3 = 112.4(1)° and N3−C−N4 = 111.2(1)°), further enforcing the interaction between the Zn atoms and N3. The Zn···Zn separation of 3.7916(5) Å is considerably smaller than that in an $EtSO_2$-bridged dimeric Zn complex (4.98 Å).[5] Likewise, this might be explained by attracting forces between the pyridylene bridge and both Zn atoms.

Polymerization Experiments. The alternating copolymerizations of CHO and CO_2 have been performed under standard conditions that are comparable to earlier work (polymerization in neat CHO of 60 °C, metal/monomer ratio = 1/1000, 10 bar CO_2 pressure).[4b,10] A summary of the results for several catalysts can be found in Table 1.

Use of the heteroleptic complex PARA-$[CaN(SiMe_3)_2 \cdot THF]_2$ as a potential catalyst in the CHO/CO_2 copolymerization did not give polymeric products, at least not under standard conditions. Hitherto it is not clear whether bimetallic calcium complexes are a priori not active or if the initiation of the polymerization reaction by the amide $(Me_3Si)_2N^-$ ion is troublesome. Analogue (β-diketiminate)$ZnN(SiMe_3)_2$ catalysts initiate the polymerization reaction by insertion of CO_2 to form the carbamate (β-diketiminate)$ZnO_2CN(SiMe_3)_2$, which rearranges via a 1,3-shift of the Me_3Si group to the true initiator (β-diketiminate)$ZnOSiMe_3$ and $O{=}C{=}N{-}SiMe_3$.[4c] Because the (β-diketiminate)$ZnN(i\text{Pr})_2$ catalyst is not active in CHO/CO_2 copolymerization and only reacts to (β-diketiminate)$ZnO_2CN(i\text{Pr})_2$,[18] this rearrangement is essential for activity. Since it is not clear if such rearrangements are also operative in calcium chemistry, we also ran polymerizations in which the PARA-$[CaN(SiMe_3)_2 \cdot THF]_2$ catalyst was pretreated with two equivalents of *i*PrOH (at −80 °C). This should give in situ formation of the bimetallic calcium alkoxide initiator PARA-$[CaO i\text{Pr} \cdot (THF)_x]_2$. However, under no circumstance could we isolate significant amounts of polymer. We are currently investigating why calcium catalysts fail to produce polymer.

Although monomeric β-diketiminate ethylzinc complexes do not initiate the CHO/CO_2 copolymerization, fair-to-good activity has been observed for the bimetallic catalysts PARA-$(ZnEt)_2$ and META-$(ZnEt)_2$ (Table 1, entries 1−2); polymers with a high content of carbonate linkages could be isolated. The striking inactivity of monometallic ethylzinc complexes can be explained by the incapability of the ethyl groups to bridge between two Zn atoms, thus inhibiting formation of catalytically active bimetallic zinc complexes. Also, CO_2 does not insert in the Et-Zn bond to give a dimeric complex with bridging carboxylate anions.[19] Only activation of the Et-Zn bond by SO_2 insertion has been shown to give an active dimeric system with bridging $EtSO_2$-moieties.[5] PARA-$(ZnEt)_2$ and META-$(ZnEt)_2$ are active without SO_2 activation on account of their bimetallic nature. A similar observation has been made for the bimetallic catalyst **2**; in this case the ethylzinc species is even a better initiator than the ethylsulfinate complex.[10]

The activity of META-$(ZnEt)_2$ is substantially higher than that of the corresponding PARA-$(ZnEt)_2$ complex. This shows the effect of the metal···metal distance on the transition states and the importance of its modulation by ligand design. The polymer obtained with PARA-$(ZnEt)_2$ has a bimodal molecular weight (MW) distribution with a rather high PDI of 3.28. Polymerization with the META-$(ZnEt)_2$ catalyst is much more controlled, and polymer with a narrow MW distribution is obtained (PDI = 1.32). Whereas the META-$(ZnEt)_2$ catalyst showed high activity, no activity was found for catalyst PYR-$(ZnEt)_2$ (not even after prolonged reaction times, entry 3 in Table 1). As both catalysts are *meta*-bridged β-diketiminate ethylzinc species, this striking difference should be explained by the presence of the N heteroatom. Partial intramolecular coordination of the central nitrogen atom to both Zn atoms might reduce their Lewis-acidity, thus inhibiting CHO coordination (the resting state of the catalyst PYR-$(ZnO_2CR)_2$ should be structurally similar to PYR-$(ZnO_2SEt)_2$, shown in Figure 6). Another explanation might involve the conformation of the bimetallic catalyst. N-Aryl-substituted β-diketiminate ligands typically show structures in which the aryl plane and the N−C−C−C−N plane are never coplanar on account of repulsion with the Me substituent in the backbone. A pyridyl substituent, however, allows this planar conformation, which might be even favored on account of intramolecular C−H···N interactions (**7**).

---

(17) Prust, J.; Stasch, A.; Zheng, W.; Roesky, H. W.; Alexopoulos, E.; Usón, I.; Böhler, D.; Schuchardt, T. *Organometallics* **2001**, *20*, 3825–3828.

(18) Chisholm, M. H.; Gallucci, J.; Phomphrai, K. *Inorg. Chem.* **2002**, *41*, 2785–2794.

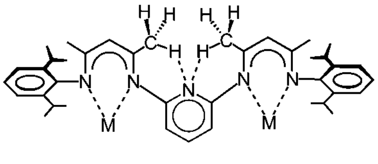

7

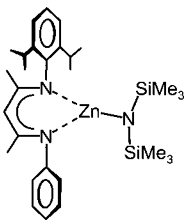

8

In fact, a similar conformation was found to be very stable for a Zn complex with the earlier mentioned 2,6-pyridylene bridged *bis*(salicylaldimide) ligand.[15] A planar arrangement like in **7** could inhibit the catalyst activity by separation of the metal centers or by alteration of the electronic properties of the β-diketiminate unit by the electron-withdrawing pyridyl bridge. Because electron-withdrawing substituents generally increase the activity,[4] the latter seems less likely.

Although the ethylzinc functionality turned out to be an efficient initiator in a bimetallic environment, increased polymer yields could be obtained with $(Me_3Si)_2N^-$ as an initiating group (entries 4−5 in Table 1). Under these circumstances the polymerization with the PARA-bridged catalyst is also more controlled (PDI = 1.48). The same trends in activity are observed: META-$[ZnN(SiMe_3)_2]_2$ > PARA-$[ZnN(SiMe_3)_2]_2$, and PYR-$[ZnN(SiMe_3)_2]_2$ is not active. Catalysts with $EtSO_2^-$ as initiating group did not improve these results, and again PYR-$[ZnO_2SEt]_2$ is not active (entries 6−7 in Table 1).

The effect of temperature was studied for the most active catalyst META-$[ZnN(SiMe_3)_2]_2$ (entries 8−10 in Table 1). Lowering the temperature from 60 °C (standard conditions) to 40 °C and, finally, to 20 °C shows, not unexpectedly, gradual lowering of isolated yields (and therefore reduced TON/TOF values), shortening of polymer chains, and narrowing of the MW distribution. The percentage of polycarbonate linkages remains the same under all conditions. Increasing the polymerization temperature from 60 to 80 °C, however, does not result in further increase of the yield. It should be mentioned that in the later stage of these polymerization experiments, reaction mixtures are highly viscous (nearly glassy), making magnetic stirring impossible. Therefore, polymer yields might be controlled by mass-transfer problems rather than by other factors. The yield of 2.04 g, which has been obtained in three independent polymerization runs (entries 5−6 and 10), might be the maximum yield on account of high viscosity. Increasing the polymerization time from 2 to 42 h (entry 11) indeed gave a hardly improved yield (2.37 g). Interestingly, polymer obtained after prolonged reaction times shows a much lower content of carbonate linkages (indicative for CO_2 transport problems) and a broad MW-distribution with a shoulder in the low MW-range (indicative of an inhomogeneous system). Viscosity as a limiting factor for polymer yield has been discussed before.[7−9]It should be noticed that such viscosity problems especially play a role for bimetallic systems: the connection of catalytic centers also connects two polymer chains essentially doubling the molecular weight of the propagating species with respect to a mononuclear catalyst.

Viscosity problems can be avoided by dilution of the reaction mixture. For monometallic zinc catalysts, dilution of the reaction mixture with CHO monomer, that is, reduction of the catalyst concentration, results in reduced polymer yields (likely on account of steering the monomer−dimer equilibrium to the less active monomeric species).[9] Bimetallic systems do not suffer from this problem and also show good conversion under diluted conditions.[7,11] Dilution of the reaction mixture with toluene indeed gave a much higher polymer yield (entry 12) than the maximum yields obtained in neat CHO. Under these diluted conditions, the $EtSO_2$-group is a better initiatior than the $(Me_3Si)_2N$-group and conversion up to 87% could be achieved (entry 13). Runs in which dilution of the reaction mixture was achieved by a reduction of the Zn/CHO ratio (instead of by addition of toluene) likewise gave improved absolute polymer yields (entry 14; because relative yields are based on CHO, these are lower). Extending the polymerization time under these diluted conditions allowed access to high-MW polycarbonates (>100 000) with a narrow MW distribution and essentially only carbonate linkages (entry 15).

The results discussed above are a clear indication of bimetallic action. To supply additional evidence for the observed synergetic effects of two adjacent Zn centers, we ran polymerizations with comparable monozinc complexes. Results obtained for polymerization with one of the best monometallic catalysts (**5**; entry 16) are comparable to those reported earlier.[4b] The yield of polymer for catalyst **5** is slightly higher than that obtained with the similar but bimetallic catalyst: META-$[ZnN(SiMe_3)_2]_2$ (entry 5). It seems that under exactly comparable conditions (temperature, pressure, reaction times, reactor, and stirring) a yield slightly higher than the earlier observed 2.04 g limit can be obtained. This might be due to a somewhat lower viscosity for reaction mixtures with monometallic catalysts; bimetallic propagating species have a higher average MW than monometallic propagating species, even when the latter are in monomer−dimer equilibrium. As is typical for the monometallic catalysts, moderate dilution of the reaction mixture with toluene gave a significant cut-back in the polymer yield (entry 17).

Because the bridge in the bimetallic catalyst does not contain bulky *i*Pr substituents (which are known to improve catalyst activity), the asymmetric catalyst **8** would be a better monometallic model for META-$[ZnN(SiMe_3)_2]_2$. This catalyst clearly shows a much lower polymer yield (entry 18) in comparison to the *meta*-bridged bimetallic system (entry 5). Therefore, connection of two (β-diketiminate)$ZnN(SiMe_3)_2$ through a *meta*-phenylene bridge improves the activity of the catalyst significantly (even despite its more severe viscosity problems).

Conclusions

A series of dinucleating *bis*(β-diketiminate) ligands with rigid bridges is easily accessible. Binuclear calcium amide reagents could only be obtained with the *para*-phenylene bridge: PARA-$[CaN(SiMe_3)_2 \cdot THF]_2$. Attempted isolation of similar calcium amide reagents with *meta*-phenylene or 2,6-pyridylene bridges gave exlusively the bimetallic homoleptic complexes (META-Ca)$_2$ and (PYR-Ca)$_x$. However, for Zn the whole series of bimetallic ethyl or amide complexes could be obtained and ligand exchange processes are not an issue.

PARA-$[CaN(SiMe_3)_2 \cdot THF]_2$ is not active in the CHO/CO_2 copolymerization; however, various zinc complexes were found to be efficient catalysts. The activity is highly dependent on the nature of the bridging unit. The *meta*-phenylene bridged catalysts are superior to the *para*-phenylene bridged systems. This noticeable difference is likely due to the differences in Zn···Zn distances. Another explanation for the much better activity of the *meta*-bridged catalyst might be the formation of an advantageous reaction pocket (the structure shown in Figure 6 could be a model for the resting state). The 2,6-pyridylene bridged catalyst showed essentially no activity. This might be

---

(19) Tang, Y.; Kassel, W. S.; Zakharov, L. N.; Rheingold, A. L.; Kemp, R. A. *Inorg. Chem.* **2005**, *44*, 359–364.

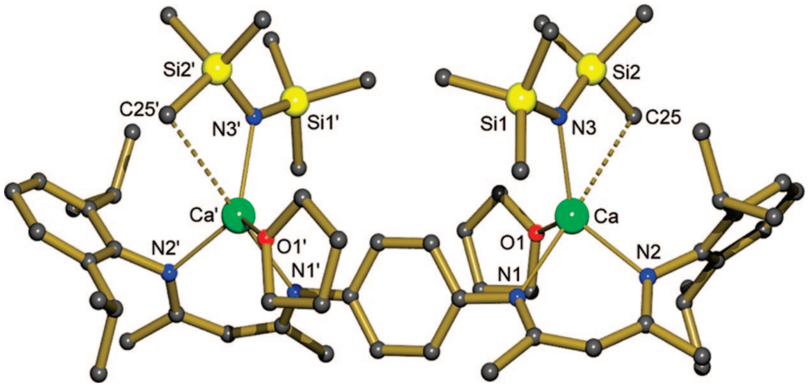

Figure 2. Crystal structure of PARA-$[CaN(SiMe_3)_2 \cdot THF]_2$ (viewed perpendicular on the vertically oriented C_2-axis). For clarity, hydrogen atoms have been omitted. Selected bond distances in Å: Ca−N1 2.368(2), Ca−N2 2.356(2), Ca−N3 2.300(2), Ca−O1 2.362(2), Ca···C25 3.315(4), and Ca···Ca′ 7.8409(8).

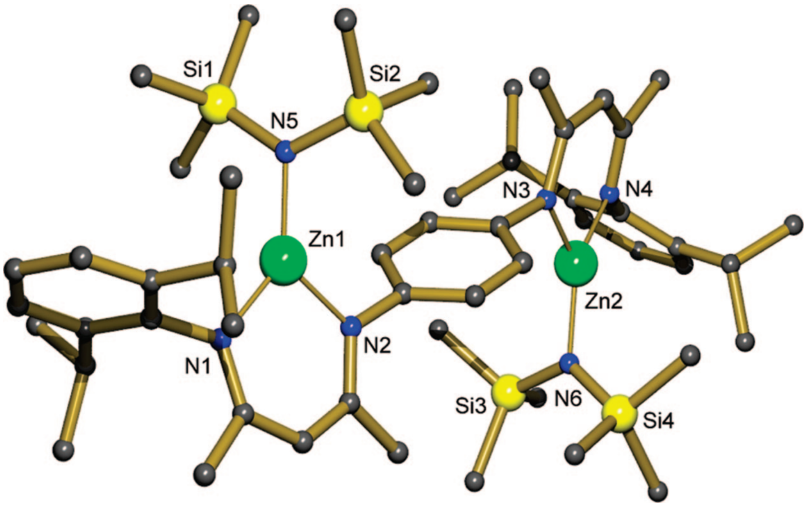

Figure 3. Crystal structure of PARA-$[ZnN(SiMe_3)_2]_2$. For clarity, hydrogen atoms have been omitted. Selected bond distances in Å: Zn1−N1 1.947(2), Zn1−N2 1.952(2), Zn1−N5 1.882(2), Zn2−N3 1.945(2), Zn2−N4 1.949(2), Zn2−N6 1.887(2), and Zn1···Zn2 8.173(2).

due to either additional coordination of the pyridyl base to the metal centers or a higher degree of conformational freedom on account of changing a CH fragment for N. Differences in electronic effects are also not ruled out.

Bimetallic action is an important aspect of these dinuclear Zn catalysts. First of all, the ethylzinc systems PARA-$(ZnEt)_2$ and META-$(ZnEt)_2$ initiate CHO/CO_2 copolymerization, whereas monometallic ethylzinc catalysts are not reactive. Second, the bimetallic zinc catalysts are also highly active under diluted conditions, whereas monometallic systems show a drastic loss of activity upon dilution. Finally, the bimetallic catalyst META-$[ZnN(SiMe_3)_2]_2$ shows a significantly higher activity than a comparable monometallic model system (**8**).

Experimental Section

General Procedures. All experiments were carried out under argon atmosphere using freshly dried solvents and standard Schlenk line and glovebox techniques. The ligands PARA-H_2, META-H_2, and PYR-H_2 have been prepared via a procedure similar to that for an earlier reported ethylene-bridged *bis*(β-diketiminate) ligand.[20] $[(Me_3Si)_2N]_2Ca \cdot (THF)_2$,[21] $[(Me_3Si)_2N]_2Zn$,[22] and 2-(2,6-diisopropylphenyl)amino-2-pentene-4-(phenyl)imine[23] were prepared according to the literature. SO_2 was dried by passing it through a column of P_4O_{10} and was condensed at −30 °C in a Schlenk tube. Et_3N was dried over CaH_2. Cyclohexene oxide was vacuum-distilled over KH and stored in a glovebox prior to use. ^1H and ^{13}C NMR spectra were recorded on a Bruker DPX300 spectrometer operating at 300 and 75.5 MHz, respectively. Molecular weight distributions of the polycarbonates were determined by GPC versus polystyrene standards using chloroform as eluent at 25 °C. Crystals were measured on a Siemens Smart diffractometer with APEXII area detector system.

Synthesis of 2-Hydroxy-4-(2,6-diisopropylphenyl)imino-2-Pentene. 2,6-Diisopropylaniline (40.0 g, 201 mmol), 2,4-pentanedione (40.0 g, 400 mmol), and montmorillonite K10 (15 g) were stirred at room temperature for 90 h. The suspension was diluted with 100 mL of CH_2Cl_2, separated from the solid material, and dried over $MgSO_4$. After removing the excess of 2,4-pentanedione under vacuum at 80 °C for several hours, a white solid was obtained in quantitative yield.

Anal. Calcd for $C_{17}H_{25}NO$ (259.39): C, 78.72; H, 9.71. Found: C, 78.58; H, 9.88. Mp: 49 °C. ^1H NMR (300 MHz, $CDCl_3$): δ

---

[20] Vitanova, D. V.; Hampel, F.; Hultzsch, K. C. *Dalton Trans.* **2005**, *9*, 1565.

[21] Westerhausen, M. *Inorg. Chem.* **1991**, *30*, 96.

[22] Darensbourg, D. J.; Holtcamp, M. W.; Struck, G. E.; Zimmer, M. S.; Niezgoda, S. A.; Rainey, P.; Robertson, J. B.; Draper, J. D.; Reibenspies, J. H. *J. Am. Chem. Soc.* **1999**, *121*, 107.

[23] Yao, Y.; Xue, M.; Luo, Y.; Zhang, Z.; Jiao, R.; Zhang, Y.; Shen, Q.; Wong, W.; Yu, K.; Sun, J. *J. Organomet. Chem.* **2003**, *678*, 108.

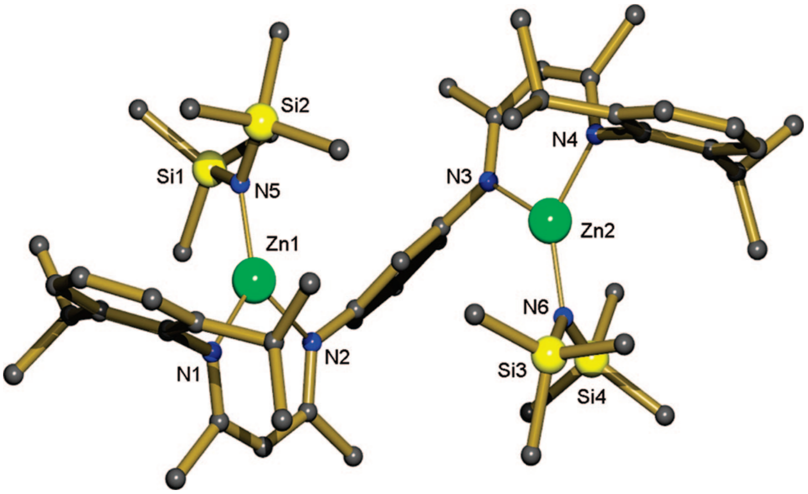

Figure 4. Crystal structure of META-[ZnN(SiMe$_3$)$_2$]$_2$. For clarity, hydrogen atoms have been omitted. Selected bond distances in Å: Zn1−N1 1.950(5), Zn1−N2 1.964(5), Zn1−N5 1.898(4), Zn2−N3 1.949(5), Zn2−N4 1.946(5), Zn2−N6 1.878(4), and Zn1···Zn2 6.098(2).

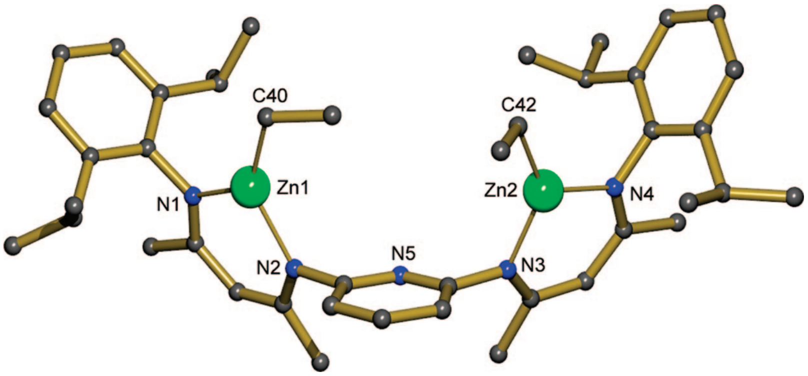

Figure 5. Crystal structure of PYR-(ZnEt)$_2$. For clarity, hydrogen atoms have been omitted. Selected bond distances in Å: Zn1−N1 1.968(2), Zn1−N2 1.974(2), Zn1−C40 1.955(3), Zn2−N3 1.962(2), Zn2−N4 1.969(2), Zn2−C42 1.961(3), and Zn1···Zn2 6.4754(4).

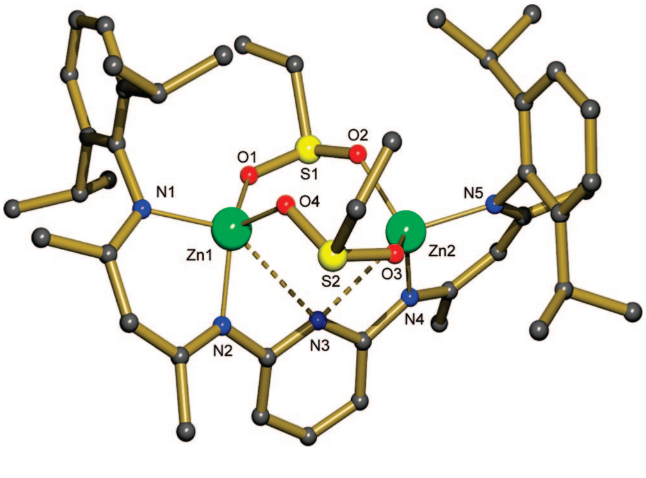

Figure 6. Crystal structure of PYR-(ZnO$_2$SEt)$_2$. For clarity, hydrogen atoms have been omitted. Selected bond distances in Å: Zn1−N1 1.998(2), Zn1−N2 1.966(3), Zn1−O1 1.936(2), Zn1−O4 1.986(2), Zn1···N3 2.841(3), Zn2−N4 1.960(3), Zn2−N5 2.008(3), Zn2−O2 1.971(2), Zn2−O3 1.945(2), Zn2···N3 2.693(3), and Zn1···Zn2 3.7916(5).

1.25 (d, $^3J_{\mathrm{H-H}} = 6.7$ Hz, 6H, CH(CH_3)$_2$), 1.32 (d, $^3J_{\mathrm{H-H}} = 6.8$ Hz, 6H, CH(CH_3)$_2$), 1.75 (s, 3H, CH_3C(N)), 2.21 (s, 3H, CH_3C(OH)), 3.14 (m, 2H, CH(CH$_3$)$_2$), 5.36 (s, 1H, CH$_3$C(OH)CH), 7.26−7.42 (m, 3H, C$H_{\mathrm{N\text{-}aryl}}$), 12.2 (s, 1H, O$H$). ^{13}C NMR (75 MHz, CDCl$_3$): δ 19.2 (CH$_3$CN), 22.7 (CH(CH$_3$)$_2$), 24.6 (CH(CH$_3$)$_2$), 28.5 (CH(CH$_3$)$_2$), 29.1 (CH$_3$COH), 95.6 (CH$_3$C(OH)CH), 123.5 (CH$_{\mathrm{N\text{-}aryl}}$), 128.2 ($CH_{\mathrm{N\text{-}aryl}}$), 133.5 ($C_q$), 146.3 ($C_q$), 163.3 ($C_q$), 195.9 (CH$_3$$C$OH).

Synthesis of PARA-H$_2$. Triethyloxonium tetrafluoroborate (18.2 g, 85.2 mmol) dissolved in 20 mL of dichloromethane was added over a period of 25 min to a stirred solution of 2-hydroxy-4-(2,6-diisopropylphenyl)imino-2-pentene (20.0 g, 77.1 mmol) in 100 mL of dichloromethane under an argon atmosphere. The mixture was stirred overnight. An equimolar portion of dry triethylamine (8.62 g, 85.2 mmol) was slowly added to the red-brown solution. After being stirred for another 20 min, a suspension of *p*-phenylenediamine (4.17 g, 38.6 mmol) in 16 mL of triethylamine was added to the mixture. The mixture was stirred for 60 h at ambient temperature. All volatiles were removed in vacuum, and the crude product was washed with acetone to yield PARA-H$_2$ as a yellow powder: 12.4 g, 54%.

Anal. Calcd for $C_{40}H_{54}N_4$ (590.90): C, 81.31; H, 9.21. Found: C, 81.30; H, 9.48. Mp: 237 °C. ^{1}H NMR (300 MHz, C$_6$D$_6$): δ 1.14 (d, $^3J_{\mathrm{H-H}} = 6.8$ Hz, 12H, CH(CH_3)$_2$), 1.18 (d, $^3J_{\mathrm{H-H}} = 6.9$ Hz, 12H, CH(CH_3)$_2$), 1.73 (s, 6H, CH_3CN), 1.83 (s, 6H, CH_3CN), 3.18 (m, 4H, CH(CH$_3$)$_2$), 4.85 (s, 2H, CH$_3$CNCH), 6.86 (s, 4H, C$H_{\mathrm{N\text{-}aryl}}$), 7.15 (s, 6H, C$H_{\mathrm{N\text{-}aryl}}$), 13.2 (s, 2H, N$H$). ^{13}C NMR (75 MHz, C$_6D_6$): δ 21.0 (CH$_3$CN), 21.5 (CH$_3$CN), 23.2 (CH(CH$_3$)$_2$), 24.7 (CH(CH$_3$)$_2$), 29.1 (CH(CH$_3$)$_2$), 96.8 (CH$_3$CNCH), 123.8 (CH$_{\mathrm{N\text{-}aryl}}$), 124.1 ($CH_{\mathrm{N\text{-}aryl}}$), 125.4 ($CH_{\mathrm{N\text{-}aryl}}$), 140.5 ($C_q$), 141.3 ($C_q$), 143.7 ($C_q$), 157.5 ($C_q$), 163.9 ($C_q$).

Synthesis of META-H$_2$. This compound was synthesized according to the same procedure as described for PARA-H$_2$. It was

Table 1. Summary of Results for the Cyclohexene Oxide/CO_2 Copolymerization[a]

entry	catalyst	*t* (h)	*T* (°C)	*P* (bar)	TON[b]	TOF[c]	isolated yield	M_n($\times 10^{-3}$)/PDI	carbonate linkages (%)[d]
1	PARA-$(ZnEt)_2$	2	60	10	72	36	0.41 g, 7.2%	14.2/3.28 bimodal	>99
2	META-$(ZnEt)_2$	2	60	10	257	129	1.50 g, 27%	98.7/1.32	98
3	PYR-$(ZnEt)_2$	17	60	10					
4	PARA-$[ZnN(SiMe_3)_2]_2$	2	60	10	127	63	0.75 g, 13%	37.7/1.48	97
5	META-$[ZnN(SiMe_3)_2]_2$	2	60	10	346	173	2.04 g, 36%	74.1/1.33	97
6	META-$(ZnO_2SEt)_2$	2	60	10	363	181	2.04 g, 36%	39.4/1.28	96
7	PYR-$(ZnO_2SEt)_2$	2	60	10					
8	META-$[ZnN(SiMe_3)_2]_2$	2	20	10	113	57	0.65 g, 12%	28.2/1.19	98
9	META-$[ZnN(SiMe_3)_2]_2$	2	40	10	204	102	1.16 g, 20%	56.3/1.25	99
10	META-$[ZnN(SiMe_3)_2]_2$	2	80	10	359	179	2.04 g, 36%	75.0/1.42	98
11	META-$[ZnN(SiMe_3)_2]_2$	42	60	10	428	10	2.37 g, 43%	88.6/4.23	91
12[e]	META-$[ZnN(SiMe_3)_2]_2$	5	60	10	748	150	4.25 g, 75%	97.7/1.39	>99
13[e]	META-$(ZnO_2SEt)_2$	5	60	10	866	173	4.95 g, 87%	89.6/1.56	>99
14[f]	META-$(ZnO_2SEt)_2$	2	60	10	525	262	3.00 g, 18%	45.7/1.28	>99
15[f]	META-$(ZnO_2SEt)_2$	6	60	10	1196	199	6.94 g, 41%	110/1.33	>99
16	**5**	2	60	10	416	208	2.34 g, 41%	86.7/1.23	96
17[g]	**5**	2	60	10	202	101	1.14 g, 20%	54.8/1.24	95
18	**8**	2	60	10	239	120	1.35 g, 24%	74.5/1.37	97

[a] Standard conditions: neat CHO (3.93 g, 40.0 mmol) with 20.0 μmol of a bimetallic catalyst or 40.0 μmol of a monometallic catalyst (metal/CHO = 1/1000). [b] The turnover number (TON) is defined as the average number of combined CHO/CO_2 insertions per metal center. [c] The turnover frequency (TOF) is defined here as TON/hour. [d] The percentage of carbonate linkages has been determined by NMR. [e] Reaction mixture diluted with toluene: metal/CHO/toluene = 1/1000/2000. [f] Metal/CHO = 1/3000. [g] Reaction mixture diluted with toluene: metal/CHO/toluene = 1/1000/1000.

purified by crystallization of the crude product, a white solid, from ethanol at −28 °C: 10.1 g, 44%.

Anal. Calcd for $C_{40}H_{54}N_4$ (590.90): C, 81.31; H, 9.21. Found: C, 81.26; H, 9.28. Mp: 139 °C. ^1H NMR (300 MHz, C_6D_6): δ 1.11 (d, $^3J_{H-H} = 6.8$ Hz, 12H, CH(CH_3)$_2$), 1.19 (d, $^3J_{H-H} = 7.0$ Hz, 12H, CH(CH_3)$_2$), 1.64 (s, 6H, CH_3CN), 1.87 (s, 6H, CH_3CN), 3.17 (m, 4H, CH(CH$_3$)$_2$), 4.84 (s, 2H, CH$_3$CNCH), 6.68 (d, $^3J_{H-H} =$ 2.0 Hz, 1H, C$H_{\text{N-aryl}}$), 6.71 (d, $^3J_{H-H} = 2.0$ Hz, 1H, C$H_{\text{N-aryl}}$), 6.78 (dd, 1H, C$H_{\text{N-aryl}}$), 7.02 (t, $^3J_{H-H} = 7.9$ Hz, 1H, C$H_{\text{N-aryl}}$), 7.15 (s, 6H, C$H_{\text{N-aryl}}$), 13.1 (s, 2H, NH). ^{13}C NMR (75 MHz, C_6D_6): δ 21.2 (CH$_3$CN), 21.3 (CH$_3$CN), 23.1 (CH(CH$_3$)$_2$), 24.7 (CH(CH$_3$)$_2$), 29.1 (CH(CH$_3$)$_2$), 97.1 (CH$_3$CNCH), 116.8 (CH$_{\text{N-aryl}}$), 117.8 (CH$_{\text{N-aryl}}$), 123.8 (CH$_{\text{N-aryl}}$), 125.7 (CH$_{\text{N-aryl}}$), 130.0 (CH$_{\text{N-aryl}}$), 141.7 (C_q), 143.0 (C_q), 146.4 (C_q), 157.9 (C_q), 163.2 (C_q).

Synthesis of PYR-H$_2$. This compound was synthesized according to the same procedure as described for PARA-H$_2$. Crystallization by cooling a hot, saturated ethanol solution to room temperature gave the product as a yellow solid: 9.6 g, 42%.

Anal. Calcd for $C_{39}H_{53}N_5$ (591.89): C, 79.14; H, 9.03. Found: C, 79.48; H, 9.13. Mp: 163 °C. ^1H NMR (300 MHz, C_6D_6): δ 1.25 (d, $^3J_{H-H} = 6.8$ Hz, 12H, CH(CH_3)$_2$), 1.26 (d, $^3J_{H-H} = 6.9$ Hz, 12H, CH(CH_3)$_2$), 1.68 (s, 6H, CH_3CN), 2.40 (s, 6H, CH_3CN), 3.12 (m, 4H, CH(CH$_3$)$_2$), 4.89 (s, 2H, CH$_3$CNCH), 6.21 (d, $^3J_{H-H} =$ 7.9 Hz, 2H, C$H_{\text{N-aryl}}$), 6.92 (t, $^3J_{H-H} = 7.9$ Hz, 1H, C$H_{\text{N-aryl}}$), 7.21−7.28 (m, 6H, C$H_{\text{N-aryl}}$), 13.8 (s, 2H, NH). ^{13}C NMR (75 MHz, C_6D_6): δ 22.3 (CH$_3$CN), 23.4 (CH(CH$_3$)$_2$), 24.8 (CH(CH$_3$)$_2$), 29.4 (CH(CH$_3$)$_2$), 100.5 (CH$_3$CNCH), 107.0 (CH$_{\text{N-aryl}}$), 124.0 (CH$_{\text{N-aryl}}$), 124.9 (CH$_{\text{N-aryl}}$), 139.0 (CH$_{\text{N-aryl}}$), 139.9 (C_q), 146.4 (C_q), 152.3 (C_q), 154.9 (C_q), 167.4 (C_q).

Synthesis of PARA-[CaN(SiMe$_3$)$_2$·THF]$_2$. A solution of PARA-H$_2$ (1.30 g, 2.20 mmol) and $[(Me_3Si)_2N]_2Ca\cdot(THF)_2$ (4.21 g, 8.33 mmol) dissolved in 12 mL of benzene was heated for 7 h at 70 °C. After evaporation of the solvent, the yellow-brown solid was washed three times with hexane and dried in vacuum to give an essentially pure crude product: 1.62 g, 65%. Colorless crystals suitable for X-ray analysis could be obtained by cooling a concentrated benzene solution to 7 °C.

Anal. Calcd for $C_{60}H_{104}Ca_2N_6O_2Si_4$ (1134.04): C, 63.55; H, 9.24. Found: C, 63.03; H, 9.12. Mp: 108 °C (dec). ^1H NMR (300 MHz, C_6D_6): δ 0.23 (s, 36H, Si(CH_3)$_3$), 1.16 (m, 8H, THF), 1.20 (d, $^3J_{H-H}$ = 6.8 Hz, 12H, CH(CH_3)$_2$), 1.30 (d, $^3J_{H-H} = 6.8$ Hz, 12H, CH(CH_3)$_2$), 1.77 (s, 6H, CH_3CN), 1.96 (s, 6H, CH_3CN), 3.20−3.28 (m, 12H, CH(CH$_3$)$_2$ + THF), 4.92 (s, 2H, CH$_3$CNCH), 7.09−7.15 (m, 10H, C$H_{\text{N-aryl}}$). ^{13}C NMR (75 MHz, C_6D_6): δ 6.23 (Si(CH$_3$)$_3$), 24.1 (CH$_3$CN), 24.6 (CH(CH$_3$)$_2$), 24.9 (CH$_3$CN), 25.2 (THF), 25.4 (CH(CH$_3$)$_2$), 28.8 (CH(CH$_3$)$_2$), 69.3 (THF), 96.8 (CH$_3$CNCH), 124.6 (CH$_{\text{N-aryl}}$), 125.0 (CH$_{\text{N-aryl}}$), 125.3 (CH$_{\text{N-aryl}}$), 141.8 (C_q), 147.0 (C_q), 163.8 (C_q), 166.6 (C_q).

Synthesis of (META-Ca)$_2$. A solution of META-H$_2$ (1.14 g, 1.93 mmol) and $[(Me_3Si)_2N]_2Ca\cdot(THF)_2$ (974 mg, 1.93 mmol) dissolved in 10 mL of benzene was heated overnight at 70 °C. A slight precipitate formed that was removed by centrifugation. The solvent was removed under vacuum, and the remaining yellow-brown solid was crystallized from a hot hexane solution. Cooling to 5 °C gave yellow crystals suitable for X-ray analysis: 1.62 g, 65%. Anal. Calcd for $C_{80}H_{104}Ca_2N_8$ (1257.93): C, 76.39; H, 8.33. Found: C, 75.93; H, 8.18. Mp: 152 °C (dec). ^1H NMR analysis of the product dissolved in benzene showed over a large temperature range extremely broad lines. Therefore, the composition of the product was checked by hydrolysis of the complex in CD_3OD, which gave essentially the starting material (META-D$_2$).

Synthesis of (PYR-Ca)$_x$. PYR-H$_2$ (867 mg, 1.47 mmol) and $[(Me_3Si)_2N]_2Ca\cdot(THF)_2$ (760 mg, 1.50 mmol) were dissolved in 10 mL of benzene. After 2 h at room temperature the reaction is completed, and the solvent was removed in vacuum. Cooling a concentrated hexane solution to −80 °C gave white crystals: 1.24 g, 67%. Anal. Calcd for $C_{78}H_{102}Ca_2N_{10}$ (1259.91): C, 74.36; H, 8.16. Found: C, 74.13; H, 7.89. Mp: 116 °C (dec). Similar to that described for (META-Ca)$_2$, ^1H NMR analysis of the product dissolved in benzene showed over a large temperature range extremely broad lines. Therefore, the composition of the product was checked by hydrolysis of the complex in CD_3OD, which gave essentially the starting material (PYR-D$_2$).

Synthesis of PARA-(ZnEt)$_2$. A suspension of PARA-H$_2$ (1.57 g, 2.64 mmol) and diethyl zinc (1 M in hexane, 4.04 g, 5.56 mmol) in 12 mL of benzene was stirred at ambient temperature for 22 h. After removing the solvent under vacuum, pure PARA-(ZnEt)$_2$ was obtained in quantitative yield. Light colored yellow crystals suitable for X-ray analysis could be obtained by slowly cooling a hot hexane solution to −28 °C.

Anal. Calcd for $C_{44}H_{62}N_4Zn_2$ (777.77): C, 67.94; H, 8.04. Found: C, 68.11; H, 7.82. Mp: 180 °C. ^1H NMR (300 MHz, C_6D_6): δ 0.38 (q, $^3J_{H-H} = 8.3$ Hz, 4H, CH_2CH$_3$), 1.07 (t, $^3J_{H-H} = 8.1$ Hz, 6H, CH$_2$CH_3), 1.14 (d, $^3J_{H-H} = 6.9$ Hz, 12H, CH(CH_3)$_2$), 1.17 (d, $^3J_{H-H}$ = 6.8 Hz, 12H, CH(CH_3)$_2$), 1.68 (s, 6H, CH_3CN), 1.84 (s, 6H, CH_3CN), 3.14 (m, 4H, CH(CH$_3$)$_2$), 4.95 (s, 2H, CH$_3$CNCH), 6.78 (s, 4H, C$H_{\text{N-aryl}}$), 7.11 (s, 6H, C$H_{\text{N-aryl}}$). ^{13}C NMR (75 MHz, C_6D_6): δ −1.87 (CH$_2$CH$_3$), 12.3 (CH$_2$$CH_3$), 23.3 ($CH_3$CN), 23.4 ($CH_3$CN), 23.5 (CH($CH_3$)$_2$), 24.4 (CH($CH_3$)$_2$), 28.4 ($C$H(CH$_3$)$_2$), 96.4

(CH_3CNCH), 123.8 $(CH_{N\text{-aryl}})$, 125.3 $(CH_{N\text{-aryl}})$, 126.0 $(CH_{N\text{-aryl}})$, 141.6 (C_q), 144.9 (C_q), 146.9 (C_q), 166.7 (C_q), 167.5 (C_q).

Synthesis of META-(ZnEt)$_2$. This compound was prepared according to the procedure described for PARA-(ZnEt)$_2$ and could be obtained in quantitative yield as a white powder.

Anal. Calcd for $C_{44}H_{62}N_4Zn_2$ (777.77): C, 67.94; H, 8.04. Found: C, 67.61; H, 7.83. Mp: 183 °C. ^1H NMR (300 MHz, C_6D_6): δ 0.37 (q, $^3J_{H-H} = 8.1$ Hz, 4H, CH_2CH_3), 1.04 (t, $^3J_{H-H} = 8.1$ Hz, 6H, CH_2CH_3), 1.17 (d, $^3J_{H-H} = 6.9$ Hz, 12H, $CH(CH_3)_2$), 1.18 (d, $^3J_{H-H} = 6.8$ Hz, 12H, $CH(CH_3)_2$), 1.67 (s, 6H, CH_3CN), 1.86 (s, 6H, CH_3CN), 3.15 (m, 4H, $CH(CH_3)_2$), 4.95 (s, 2H, CH_3CNCH), 6.47 (s, 1H, $CH_{N\text{-aryl}}$), 6.65 (d, $^3J_{H-H} = 7.8$ Hz, 2H, $CH_{N\text{-aryl}}$), 7.00 (t, $^3J_{H-H} = 7.9$ Hz, 1H, $CH_{N\text{-aryl}}$), 7.10 (s, 6H, $CH_{N\text{-aryl}}$). ^{13}C NMR (75 MHz, C_6D_6): δ −1.95 (CH_2CH_3), 12.4 (CH_2CH_3), 23.4 (CH_3CN), 23.4 (CH_3CN), 23.5 $(CH(CH_3)_2)$, 24.4 $(CH(CH_3)_2)$, 28.5 $(CH(CH_3)_2)$, 96.4 (CH_3CNCH), 121.0 $(CH_{N\text{-aryl}})$, 121.5 $(CH_{N\text{-aryl}})$, 123.9 $(CH_{N\text{-aryl}})$, 126.1 $(CH_{N\text{-aryl}})$, 129.5 $(CH_{N\text{-aryl}})$, 141.7 (C_q), 145.0 (C_q), 151.4 (C_q), 166.4 (C_q), 167.6 (C_q).

Synthesis of PYR-(ZnEt)$_2$. This compound was prepared according to the procedure described for PARA-(ZnEt)$_2$. The reaction times could be reduced to 1 h, and the product was obtained in quantitative yield. Colorless crystals suitable for X-ray analysis could be obtained by slowly cooling a hot hexane solution to room temperature.

Anal. Calcd for $C_{43}H_{61}N_5Zn_2$ (778.75): C, 66.32; H, 7.90. Found: C, 66.68; H, 8.24. Mp: 175 °C. ^1H NMR (300 MHz, C_6D_6): δ 0.44 (q, $^3J_{H-H} = 8.1$ Hz, 4H, CH_2CH_3), 1.04−1.14 (m, 30H, $CH_2CH_3 + CH(CH_3)_2$), 1.64 (s, 6H, CH_3CN), 2.05 (s, 6H, CH_3CN), 3.05 (m, 4H, $CH(CH_3)_2$), 4.96 (s, 2H, CH_3CNCH), 6.52 (d, $^3J_{H-H} = 7.7$ Hz, 2H, $CH_{N\text{-aryl}}$), 7.08−7.15 (m, 7H, $CH_{N\text{-aryl}}$). ^{13}C NMR (75 MHz, C_6D_6): δ −1.46 (CH_2CH_3), 12.4 (CH_2CH_3), 23.4 (CH_3CN), 23.5 $(CH(CH_3)_2)$, 23.9 (CH_3CN), 24.2 $(CH(CH_3)_2)$, 28.4 $(CH(CH_3)_2)$, 97.5 (CH_3CNCH), 114.5 $(CH_{N\text{-aryl}})$, 123.9 $(CH_{N\text{-aryl}})$, 126.1 $(CH_{N\text{-aryl}})$, 139.0 (C_q), 141.5 $(CH_{N\text{-aryl}})$, 144.8 (C_q), 161.6 (C_q), 165.7 (C_q), 168.6 (C_q).

Synthesis of PARA-[ZnN(SiMe$_3$)$_2$]$_2$. A solution of PARA-H$_2$ (1.08 g, 1.83 mmol) and $[(Me_3Si)_2N]_2Zn$ (1.46 g, 3.78 mmol) in 10 mL of benzene was heated for 8 h at 70 °C. The solution was concentrated to 3.5 mL, warmed to 70 °C, and slowly cooled to room temperature. The product crystallized in the form of light yellow large crystals: 1.08 g, 57%.

Anal. Calcd for $C_{52}H_{88}N_6Si_4Zn_2$ (1040.42): C, 60.03; H, 8.52. Found: C, 59.88; H, 8.54. Mp: 253 °C. ^1H NMR (300 MHz, C_6D_6): δ 0.01 (s, 36H, $Si(CH_3)_3$), 1.12 (d, $^3J_{H-H} = 6.8$ Hz, 12H, $CH(CH_3)_2$), 1.37 (d, $^3J_{H-H} = 6.8$ Hz, 12H, $CH(CH_3)_2$), 1.66 (s, 6H, CH_3CN), 1.93 (s, 6H, CH_3CN), 3.26 (m, 4H, $CH(CH_3)_2$), 4.87 (s, 2H, CH_3CNCH), 6.95 (s, 4H, $CH_{N\text{-aryl}}$), 7.14 (s, 6H, $CH_{N\text{-aryl}}$). ^{13}C NMR (75 MHz, C_6D_6): δ 5.13 $(Si(CH_3)_3)$, 24.0 (CH_3CN), 24.0 (CH_3CN), 24.2 $(CH(CH_3)_2)$, 24.7 $(CH(CH_3)_2)$, 28.2 $(CH(CH_3)_2)$, 96.2 (CH_3CNCH), 124.1 $(CH_{N\text{-aryl}})$, 126.0 $(CH_{N\text{-aryl}})$, 126.1 $(CH_{N\text{-aryl}})$, 142.0 (C_q), 144.0 (C_q), 145.7 (C_q), 168.3 (C_q), 169.4 (C_q).

Synthesis of META-[ZnN(SiMe$_3$)$_2$]$_2$. A solution of META-H$_2$ (918 mg, 1.55 mmol) and $[(Me_3Si)_2N]_2Zn$ (1.26 g, 3.26 mmol) in 10 mL of benzene was heated overnight at 70 °C. The solution was concentrated to 3.5 mL, warmed to 70 °C, and slowly cooled to room temperature. After a few minutes META-[ZnN(SiMe$_3$)$_2$]$_2$ crystallized as colorless crystals: 823 mg, 51%.

Anal. Calcd for $C_{52}H_{88}N_6Si_4Zn_2$ (1040.42): C, 60.03; H, 8.52. Found: C, 60.24; H, 8.75. Mp: 229 °C. ^1H NMR (300 MHz, C_6D_6): δ 0.00 (s, 36H, $Si(CH_3)_3$), 1.14 (d, $^3J_{H-H} = 6.8$ Hz, 12H, $CH(CH_3)_2$), 1.38 (d, $^3J_{H-H} = 6.8$ Hz, 12H, $CH(CH_3)_2$), 1.61 (s, 6H, CH_3CN), 2.04 (s, 6H, CH_3CN), 3.24 (m, 4H, $CH(CH_3)_2$), 4.84 (s, 2H, CH_3CNCH), 6.78−6.85 (m, 3H, $CH_{N\text{-aryl}}$), 7.10−7.14 (m, 6H, $CH_{N\text{-aryl}}$). ^{13}C NMR (75 MHz, C_6D_6): δ 5.30 $(Si(CH_3)_3)$, 24.2 (CH_3CN), 24.3 (CH_3CN), 24.4 $(CH(CH_3)_2)$, 25.0 $(CH(CH_3)_2)$, 28.5 $(CH(CH_3)_2)$, 96.6 (CH_3CNCH), 122.3 $(CH_{N\text{-aryl}})$, 123.8 $(CH_{N\text{-aryl}})$, 124.3 $(CH_{N\text{-aryl}})$, 126.5 $(CH_{N\text{-aryl}})$, 128.9 $(CH_{N\text{-aryl}})$, 142.3 (C_q), 144.3 (C_q), 149.6 (C_q), 167.8 (C_q), 169.6 (C_q).

Synthesis of PYR-[ZnN(SiMe$_3$)$_2$]$_2$. A solution of PYR-H$_2$ (835 mg, 1.41 mmol) and $[(Me_3Si)_2N]_2Zn$ (1.10 g, 2.85 mmol) in 10 mL of benzene was heated for 18 h at 70 °C. The solution was concentrated to 3 mL and stored at 5 °C. After a few days PYR-[ZnN(SiMe$_3$)$_2$]$_2$ could be obtained as colorless needles: 710 mg, 49%.

Anal. Calcd for $C_{51}H_{87}N_7Si_4Zn_2$ (1041.41): C, 58.82; H, 8.42. Found: C, 58.64; H, 8.37. Mp: 188 °C. ^1H NMR (300 MHz, C_6D_6): δ 0.01 (s, 36H, $Si(CH_3)_3$), 1.11 (d, $^3J_{H-H} = 6.5$ Hz, 12H, $CH(CH_3)_2$), 1.36 (d, $^3J_{H-H} = 6.5$ Hz, 12H, $CH(CH_3)_2$), 1.61 (s, 6H, CH_3CN), 2.18 (s, 6H, CH_3CN), 3.20 (m, 4H, $CH(CH_3)_2$), 4.86 (s, 2H, CH_3CNCH), 6.77 (d, $^3J_{H-H} = 7.6$ Hz, 2H, $CH_{N\text{-aryl}}$), 7.13 (s, 6H, $CH_{N\text{-aryl}}$), 7.23 (t, $^3J_{H-H} = 7.6$ Hz, 1H, $CH_{N\text{-aryl}}$). ^{13}C NMR (75 MHz, C_6D_6): δ 5.26 $(Si(CH_3)_3)$, 24.4 $(CH(CH_3)_2)$, 24.7 (CH_3CN), 25.0 $(CH(CH_3)_2)$, 28.4 $(CH(CH_3)_2)$, 97.4 (CH_3CNCH), 116.3 $(CH_{N\text{-aryl}})$, 124.3 $(CH_{N\text{-aryl}})$, 126.6 $(CH_{N\text{-aryl}})$, 138.6 (C_q), 142.1 $(CH_{N\text{-aryl}})$, 144.1 (C_q), 159.9 (C_q), 166.7 (C_q), 170.7 (C_q).

Synthesis of META-(ZnO$_2$SEt)$_2$. An excess of SO$_2$ was condensed to a precooled (−25 °C) yellow solution of META-(ZnEt)$_2$ (938 mg, 1.21 mmol) in 15 mL of toluene. The yellow solution immediately turned deep-red and was stirred for approximately 30 min at this temperature. The cooling bath was removed, and the solution was slowly warmed to room temperature. After removal of SO$_2$ the solution turned yellow again. Solvents were removed under high vacuum. The raw product was washed three times with 10 mL portions of hexane to yield a white precipitate: 823 mg, 75%.

Anal. Calcd for $C_{44}H_{62}N_4O_4S_2Zn_2$ (905.89): C, 58.34; H, 6.90. Found: C, 57.98; H, 6.98. Mp: 258 °C (dec). ^1H NMR (300 MHz, THF-d_8): δ 0.40−0.85 (m, 6H, CH_2CH_3), 1.10 (d, $^3J_{H-H} = 6.9$ Hz, 12H, $CH(CH_3)_2$), 1.24 (d, $^3J_{H-H} = 6.7$ Hz, 12H, $CH(CH_3)_2$), 1.63 (s, 6H, CH_3CN), 2.00−2.15 (m, 4H, CH_2CH_3), 2.26 (s, 6H, CH_3CN), 3.13 (m, 4H, $CH(CH_3)_2$), 4.82 (s, 2H, CH_3CNCH), 6.65 (d, $^3J_{H-H} = 7.7$ Hz, 2H, $CH_{N\text{-aryl}}$), 7.05−7.14 (m, 7H, $CH_{N\text{-aryl}}$), 7.63 (s, 1H, $CH_{N\text{-aryl}}$). ^{13}C NMR (75 MHz, THF-d_8): δ 5.48 (CH_2CH_3), 23.7 (CH_3CN), 24.7 (CH_3CN), 25.1 $(CH(CH_3)_2)$, 25.4 $(CH(CH_3)_2)$, 28.8 $(CH(CH_3)_2)$, 54.0 (CH_2CH_3), 97.1 (CH_3CNCH), 119.5 $(CH_{N\text{-aryl}})$, 121.8 $(CH_{N\text{-aryl}})$, 124.7 $(CH_{N\text{-aryl}})$, 126.6 $(CH_{N\text{-aryl}})$, 130.0 $(CH_{N\text{-aryl}})$, 143.8 (C_q), 145.4 (C_q), 149.9 (C_q), 166.2 (C_q), 170.1 (C_q).

Synthesis of PYR-(ZnO$_2$SEt)$_2$. This compound was synthesized according to the procedure described for the preparation of META-(ZnO$_2$SEt)$_2$. After evaporation of all volatiles, the product was extracted twice with 6 mL of benzene: 538 mg, 49%. Yellow crystals suitable for X-ray analysis could be obtained by slowly cooling a hot hexane/THF (8:1) solution to −28 °C.

Anal. Calcd for $C_{43}H_{61}N_5O_4S_2Zn_2$ (906.88): C, 56.95; H, 6.78. Found: C, 56.81; H, 6.53. Mp: 235 °C (dec). ^1H NMR (300 MHz, C_6D_6): δ 0.59 (m, 6H, CH_2CH_3), 1.14 (d, $^3J_{H-H} = 6.8$ Hz, 12H, $CH(CH_3)_2$), 1.32 (d, $^3J_{H-H} = 6.5$ Hz, 12H, $CH(CH_3)_2$), 1.68 (s, 6H, CH_3CN), 2.00 (s, 6H, CH_3CN), 2.24 (m, 4H, CH_2CH_3), 3.44 (m, 4H, $CH(CH_3)_2$), 4.74 (s, 2H, CH_3CNCH), 6.18 (d, $^3J_{H-H} = 7.8$ Hz, 2H, $CH_{N\text{-aryl}}$), 6.93 (t, $^3J_{H-H} = 7.6$ Hz, 1H, $CH_{N\text{-aryl}}$), 7.08 (s, 6H, $CH_{N\text{-aryl}}$). ^{13}C NMR (75 MHz, C_6D_6): δ 6.45 (CH_2CH_3), 24.4 (CH_3CN), 24.5 $(CH(CH_3)_2)$, 25.3 $(CH(CH_3)_2)$, 25.5 (CH_3CN), 28.6 $(CH(CH_3)_2)$, 53.6 (CH_2CH_3), 99.0 (CH_3CNCH), 111.1 $(CH_{N\text{-aryl}})$, 124.4 $(CH_{N\text{-aryl}})$, 126.3 $(CH_{N\text{-aryl}})$, 138.3 (C_q), 142.8 $(CH_{N\text{-aryl}})$, 144.9 (C_q), 160.1 (C_q), 163.5 (C_q), 171.0 (C_q).

Synthesis of 8. A solution of 2-(2,6-diisopropylphenyl)amino-2-pentene-4-(phenyl)imine (512 mg, 1.53 mmol) and $[(Me_3Si)_2N]_2Zn$ (592 mg, 1.53 mmol) in 7 mL of benzene was heated for 18 h at 70 °C. The solvent was evaporated in vacuum, and the crude product was washed with two 5 mL portions of hexane to obtain **8** as a white solid: 663 mg, 82%.

Anal. Calcd for $C_{29}H_{47}N_3Si_2Zn$ (559.27): C, 62.28; H, 8.47. Found: C, 62.65; H, 8.76. Mp: 142 °C. ^1H NMR (300 MHz, C_6D_6): δ −0.01 (s, 18H, Si(CH_3)$_3$), 1.12 (d, $^3J_{H-H}$ = 6.7 Hz, 6H, CH(CH_3)$_2$), 1.35 (d, $^3J_{H-H}$ = 6.8 Hz, 6H, CH(CH_3)$_2$), 1.64 (s, 3H, CH_3CN), 1.71 (s, 3H, CH_3CN), 3.24 (m, 2H, CH(CH_3)$_2$), 4.83 (s, 2H, CH_3CNCH), 6.94−6.99 (m, 3H, $CH_{N\text{-aryl}}$), 7.12−7.14 (m, 5H, $CH_{N\text{-aryl}}$). ^{13}C NMR (75 MHz, C_6D_6): δ 5.78 (Si(CH_3)$_3$), 23.4 (CH_3CN), 24.9 (CH_3CN), 25.0 (CH(CH_3)$_2$), 25.5 (CH(CH_3)$_2$), 29.0 (CH(CH_3)$_2$), 96.9 (CH_3CNCH), 125.1 ($CH_{N\text{-aryl}}$), 125.7 ($CH_{N\text{-aryl}}$), 126.6 ($CH_{N\text{-aryl}}$), 127.1 ($CH_{N\text{-aryl}}$), 129.8 ($CH_{N\text{-aryl}}$), 142.8 (C_q), 144.8 (C_q), 149.4 (C_q), 168.6 (C_q), 170.2 (C_q).

Crystal Structure Determination. Structures have been solved and refined using the programs SHELXS-97 and SHELXL-97, respectively.[24] All geometry calculations and graphics have been performed with PLATON.[25] Crystallographic data (excluding structure factors) have been deposited with the Cambridge Crystallographic Data Centre as supplementary publication No. CCDC 692794−692799. Copies of the data can be obtained free of charge on application to CCDC, 12 Union Road, Cambridge CB21EZ, UK (fax: (+44)1223−336−033; E-mail: deposit@ccdc.cam.ac.uk).

General Procedure for the Cyclohexene Oxide/CO_2 Copolymerization. A 20.0 μmol portion of a bimetallic catalyst (or 40.0 μmol of a monometallic catalyst) was dissolved in 3.93 g (40.0 mmol) of cyclohexene oxide in a glovebox. This solution was injected into a preheated reactor (60 °C) that was immediately pressurized with CO_2 (10 bar). After the mixture was stirred at the desired temperature, pressure, and time, the mixture was cooled to ambient temperature and the CO_2 pressure was slowly released. The normally very viscous mixture was diluted with 100 mL of CH_2Cl_2. After the solution was concentrated, the polymer was precipitated by adding 100 mL of methanol, filtered off, and dried under vacuum for 5 h at 100 °C. The obtained polymer was analyzed via ^1H NMR.

Crystal Data for (META-Ca)$_2$. Measurement at −70 °C, Mo$_{K\alpha}$, θ_{max} = 24.4°, 41 637 reflections measured, 6380 independent reflections (R_{int} = 0.157), 3787 reflections observed with $I > 2\sigma(I)$, monoclinic, space group $C2/c$, a = 30.800(4), b = 16.172(2), c = 16.660(2), β = 107.606(8), V = 7909.6(17) Å^3, formula $C_{80}H_{104}Ca_2N_8 \cdot C_6H_6$, Z = 4, R = 0.0872, $wR2$ = 0.2436, GOF = 1.04, ρ_{max} = 0.74 e Å^{-3}, ρ_{min} = −0.60 e Å^{-3}. All hydrogen atoms have been placed on calculated positions and were refined in a riding mode. The somewhat poor crystal quality is due to the small size of the crystal (0.3 × 0.1 × 0.05 mm^3) and twinning problems (a penetrating second crystal lattice has been separated from the main crystal lattice).

Crystal Data for PARA-[CaN(SiMe$_3$)$_2$·THF]$_2$. Measurement at −70 °C, Mo$_{K\alpha}$, θ_{max} = 25.4°, 49 558 reflections measured, 6281 independent reflections (R_{int} = 0.075), 4038 reflections observed with $I > 2\sigma(I)$, orthorhombic, space group $Pccn$, a = 34.0276(9), b = 10.3059(3), c = 19.5596(5), V = 6859.3(3) Å^3, formula $C_{60}H_{104}Ca_2N_6O_2Si_4$, Z = 4, R = 0.0495, $wR2$ = 0.1470, GOF = 1.03, ρ_{max} = 0.25 e Å^{-3}, ρ_{min} = −0.34 e Å^{-3}. Most hydrogen atoms have been observed and were refined isotropically. The hydrogen atoms of the Me_3Si groups and the THF ligand have been placed on calculated positions and were refined in a riding mode.

Crystal Data for PARA-[ZnN(SiMe$_3$)$_2$]$_2$. Measurement at −70 °C, Mo$_{K\alpha}$, θ_{max} = 27.6°, 88 638 reflections measured, 15 599 independent reflections (R_{int} = 0.079), 10 876 reflections observed with $I > 2\sigma(I)$, monoclinic, space group $P2_1/n$, a = 18.469(4), b = 21.213(4), c = 19.522(4), β = 117.927(10), V = 6758(2) Å^3, formula $C_{52}H_{88}N_6Si_4Zn_2 \cdot (C_6H_6)_2$, Z = 4, R = 0.0397, $wR2$ = 0.1038, GOF = 0.99, ρ_{max} = 0.43 e Å^{-3}, ρ_{min} = −0.33 e Å^{-3}. All hydrogen atoms have been placed on calculated positions and were refined in a riding mode. One of the cocrystallized benzene molecules is perfectly ordered, the other was disordered and was treated with the SQUEEZE procedure incorporated in the program PLATON.[25]

Crystal Data for META-[ZnN(SiMe$_3$)$_2$]$_2$. Measurement at −80 °C, Mo$_{K\alpha}$, θ_{max} = 28.4°, 136 020 reflections measured, 17 484 independent reflections (R_{int} = 0.114), 9114 reflections observed with $I > 2\sigma(I)$, monoclinic, space group $P2_1/n$, a = 10.9191(8), b = 35.169(3), c = 18.4217(14), β = 95.451(5), V = 7042.2(10) Å^3, formula $C_{52}H_{88}N_6Si_4Zn_2 \cdot (C_6H_6)_2$, Z = 4, R = 0.0708, $wR2$ = 0.2374, GOF = 1.08, ρ_{max} = 0.72 e Å^{-3}, ρ_{min} = −0.82 e Å^{-3}. All hydrogen atoms have been placed on calculated positions and were refined in a riding mode. Both cocrystallized benzene molecules were fully disordered and were treated with the SQUEEZE procedure incorporated in the program PLATON.[25]

Crystal Data for PYR-(ZnEt)$_2$. Measurement at −70 °C, Mo$_{K\alpha}$, θ_{max} = 27.1°, 80 788 reflections measured, 9230 independent reflections (R_{int} = 0.047), 7312 reflections observed with $I > 2\sigma(I)$, triclinic, space group P-1, a = 11.6831(4), b = 14.2544(5), c = 14.5619(5), α = 67.162(2), β = 79.572(2), γ = 70.257(2), V = 2100.10(13) Å^3, formula $C_{43}H_{61}N_5Zn_2$, Z = 2, R = 0.0333, $wR2$ = 0.0878, GOF = 1.07, ρ_{max} = 0.59 e Å^{-3}, ρ_{min} = −0.64 e Å^{-3}. All hydrogen atoms have been placed on calculated positions and were refined in a riding mode.

Crystal Data for PYR-(ZnO$_2$SEt)$_2$. Measurement at −70 °C, Mo$_{K\alpha}$, θ_{max} = 25.7°, 89 534 reflections measured, 8731 independent reflections (R_{int} = 0.096), 6174 reflections observed with $I > 2\sigma(I)$, monoclinic, space group $P2_1/n$, a = 11.2229(3), b = 28.1674(8), c = 15.3663(2), β = 108.547(2), V = 4605.3(2) Å^3, formula $C_{43}H_{61}N_5O_4S_2Zn_2$, Z = 4, R = 0.0439, $wR2$ = 0.1091, GOF = 1.05, ρ_{max} = 0.63 e Å^{-3}, ρ_{min} = −0.68 e Å^{-3}. All hydrogen atoms have been placed on calculated positions and were refined in a riding mode. One of the $EtSO_2$-ligands is disordered over two positions in a 90/10 ratio. Figure 6 shows the position with highest occupation.

Acknowledgment. We are grateful to the Deutsche Forschungsgemeinschaft for financial support of this work (AM^2-net). Professor Dr. R. Boese and D. Bläser (Universität Duisburg-Essen) are thanked for collection of the X-ray diffraction data, and D. Jacobi (Universität Duisburg-Essen) is thanked for the GPC analyses.

Supporting Information Available: The cif files and ORTEP plots for all crystal structures are available as Supporting Information. This material is available free of charge via the Internet at http://pubs.acs.org.

OM800597F

---

(24) (a) Sheldrick, G. M. *SHELXS-97, Program for Crystal Structure Solution*; Universität Göttingen: Germany, 1997; (b) Sheldrick, G. M. *SHELXL-97, Program for Crystal Structure Refinement*; Universität Göttingen: Germany, 1997;.

(25) Spek, A. L. *PLATON, A Multipurpose Crystallographic Tool*; Utrecht University: Utrecht, The Netherlands, 2000.